AIP Applied Physics Letters

Model to determine the self-resonant frequency of micromachined spiral inductors

C. C. Chen, Cheng-De Lin, and Y. T. Cheng

Citation: Applied Physics Letters **89**, 103521 (2006); doi: 10.1063/1.2346371
View online: http://dx.doi.org/10.1063/1.2346371
View Table of Contents: http://scitation.aip.org/content/aip/journal/apl/89/10?ver=pdfcov
Published by the AIP Publishing

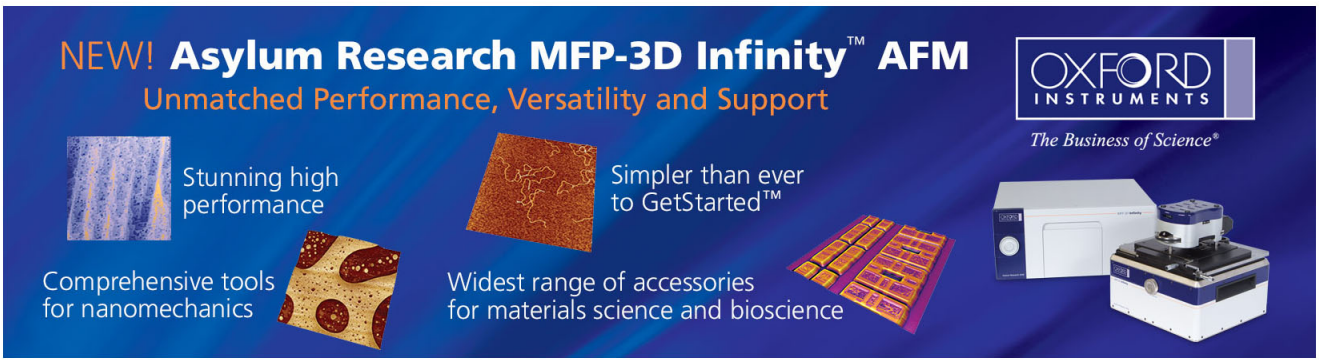

Model to determine the self-resonant frequency of micromachined spiral inductors

C. C. Chen, Cheng-De Lin, and Y. T. Cheng[a)]
Microsystems Integration Laboratory, Department of Electronics Engineering, National Chiao Tung University, Hsinchu, Taiwan 300, Republic of China

(Received 28 December 2005; accepted 24 July 2006; published online 7 September 2006)

This letter presents an approach to characterize electron behaviors within polygonal micromachined spiral inductors in which self-resonance occurs. Combining with the concepts of anomalous dispersion, standing wave, and field scattering, the self-resonant frequency of the microinductors can be calculated by means of an associated analytical model. According to this model the self-resonant frequency (SRF) can be derived as the "free electron" frequency of the inductor material. Simulation and measurement results validate that the model can provide a satisfactory prediction to the SRF of polygonal micromachined spiral inductors. © *2006 American Institute of Physics*. [DOI: 10.1063/1.2346371]

Nowadays, several methodologies were proposed for predicting the self-resonant frequency (SRF) of a spiral inductor, such as empirical curve fitting using lumped circuit parameters,[1–4] data extraction from measured *S* parameters,[5] electromagnetic field modeling,[6] and method of moments (MoM) analysis.[7] Although these approaches precisely determine the SRF, most of them are time consuming in calculation and nonphysically straightforward which could not help circuit designer to easily reach for an optimal design. In order to surmount this predicament, an analytic closed-form model based on solid-state theory is presented for predicting the SRF of polygonal spiral microinductors.

Both conceptually and physically, the self-resonant occurrence of a polygonal spiral microinductor indicates a complete stored energy transformation from magnetic energy into electrical energy, and vice versa. Being analogous with the anomalous dispersion of a conducting medium, it can be safely assumed that incident electromagnetic (EM) waves will be entirely absorbed and transformed into the kinetic energy of free electrons inside the medium. In other words, the free electrons and associated EM energy can be treated as quantized waves and energy, respectively. Thus, the averaged kinetic energy of the free electrons inside the resonating inductor can be calculated using the dispersion relation[8] as $E_L=\sqrt{3/5}(\hbar^2/m_e)(3\pi^2 n_e)^{1/3}k$, where $\hbar$, n_e, and m_e are Planck's constant, the free electron density, and electron mass in the inductor material, respectively. For copper, the free electron density and mass are 8.45×10^{28} m^{-3} and 9.11×10^{-31} kg, respectively. The factor k is the wave number of free electrons.

The wave number is a critical parameter which is closely related to the self-resonant frequency of polygonal spiral inductors. In this model, the concept of standing wave is implemented to characterize the free electron behavior while the inductor starts self-resonating. The free electrons similar to the notion of standing waves move back and forth through the terminals of the spiral inductor. Thus, the wave number k of the electron could be identified as $m\pi/l$ where m and l represent an integral number and the total length of the spiral inductor, respectively. Once the free electrons behave like standing waves, they can effectively absorb the energy of the EM wave propagating along the inductor. Meanwhile, since the operational frequency falls in a range of 1–20 GHz for most of radio frequency integrated circuits (RFICs) in which the EM wavelength is about centimeters long, the lowest mode would be the dominant one. In other words, the integral number m is equal to unity and $k=\pi/l$. Thus, the self-resonant frequency of a spiral microinductor ω_r would be equal to the frequency of the resonating electron and could be calculated as follows:

$$E_L \approx \sqrt{3/5}\frac{\hbar^2}{m_e}(3\pi^2 n_e)^{1/3}\frac{\pi}{l}. \tag{1}$$

For the most part, the hypothesis simply embodies the culmination of the analytic model.

In addition, another hypothesis is made to facilitate a mental visualization of the electron behaviors inside the polygonal spiral inductor while EM wave propagates along with the entity. Homologizing the hydromechanics that expounds the ideals about the fluidic flow through a channel with corners, it can be assumed that small free vortices would locally form in the apex of corner while electrons travel inside the polygonal spiral inductor. Since the vortex is a closed path and its diameter is much smaller than the inductor width, it is convenient to assume that the vortex is infinitesimal in this model. The electrons moving in a form of free vortex can be treated as a cluster of static electrons to build up a quasistatic electric field in the apex of the corner. Thus, according to Jackson's field theory[9] and the notion of hydromechanics, there will be electric fields built up in the neighborhood of corners while an external electric field is applied on a conducting material. To a polygonal spiral inductor with several corners in the boundary, the quasistatic electric field built up in each corner has the following form which is calculated by the variation principle:[10]

$$\mathbf{E}(r) = \frac{1}{4\pi\varepsilon_0}\frac{q[\pi+8\sin(\pi^2/4\beta)]^2}{8\beta\varpi h[\csc(\beta/2)-1](\pi+\beta)}\hat{r}, \tag{2}$$

where q is elementary charge, ϖ and h are the width and height of polygon spiral inductor, respectively, β is the corner angle, and the field is centered at the outer apex of each corner. By considering the field scattering, free electrons

a)Electronic mail: ytcheng@mail.nctu.edu.tw

move near the corner would be scattered and alter their trajectories due to the built-up electrical field in the corner. The energy lost of free electrons due to the field scattering can be calculated as follows:[11,12]

$$E_C = \frac{\pi\varepsilon_0\varpi h[\csc(\beta/2)-1]|\mathbf{E}|q}{NV^{2/3}\sqrt{\sigma_{\text{eff}}}}\csc^2\left(\frac{\pi-\beta}{2}\right)$$
$$= \frac{q^2}{4NV^{2/3}\sqrt{\sigma_{\text{eff}}}}\frac{(\pi+8\sin(\pi^2/4\beta))^2}{8\beta(\pi+\beta)}\csc^2\left(\frac{\pi-\beta}{2}\right)$$
$$\text{for } 0<\beta<\pi, \tag{3a}$$

$$E_C = \lim_{N\to\infty}\frac{q^2}{4NV^{2/3}\sqrt{\sigma_{\text{eff}}}}\frac{(\pi+4\sqrt{2})^2}{4\pi}\frac{\pi}{2.7}\int dN$$
$$\text{for } \beta=\pi(\text{circular spiral}), \tag{3b}$$

where N, V, and σ_{eff} are the number of corners, the volume of polygon spiral inductor, and the effective cross section of the inductor, respectively. Here, the effective cross sections are equal to 0.101, 0.281,[13] and 0.375 times the cross section of rectangular, octagonal, and circular inductors, respectively. The corresponding reference ground point for calculating E_C is assumed infinity. For the polygonal spiral inductors in the RFIC design, the reference ground point would usually be far away from itself. Since the previous investigation already found that the substrate coupling effects could be neglected as long as the air gap is larger than 60 μm,[14] which can be easily realized in the microinductor fabrication. Thus, it is reasonable and practical to be excused for this assumption.

After considering the energy lost in the corner field scattering, the realistic SRF, ωr, of a polygonal spiral inductor in this model should be derived as follows which is equal to the free electron frequency:

$$\omega_r = (E_L + NE_C)/\hbar \quad \text{for } 0<\beta<\pi, \tag{4a}$$

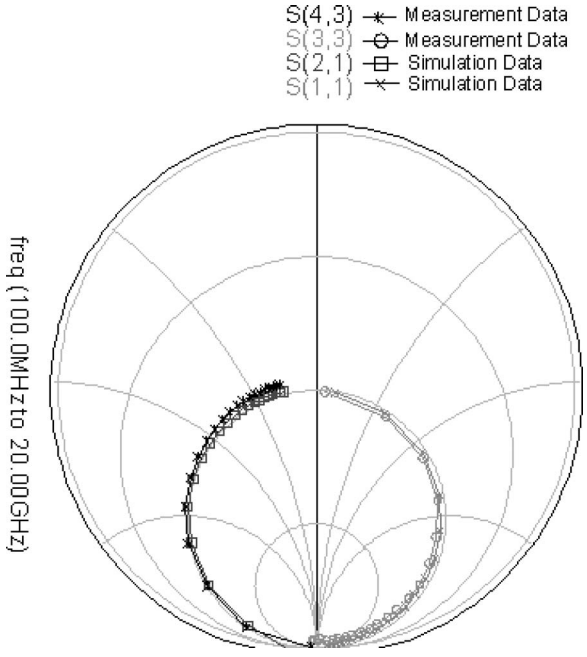

FIG. 1. Comparisons between the HFSS simulation and measurement results of the 3.5 turns, 5 μm thick suspended spiral inductor ($l_{\max}$=300 μm, ϖ=15 μm, and S=5 μm). The frequency range is from 1 to 20 GHz.

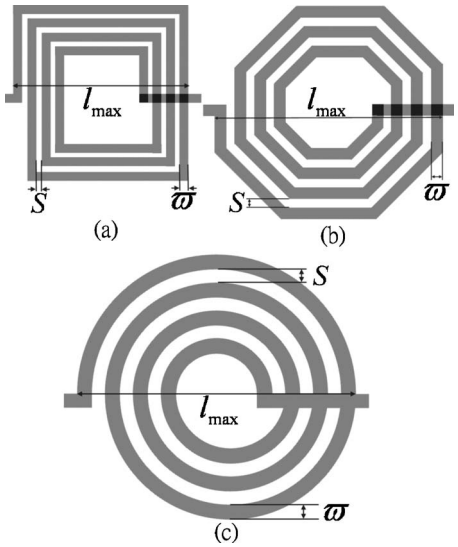

FIG. 2. Schematic diagram of the two ports spiral polygon inductor realizations: (a) rectangular, (b) octagonal, and (c) circular. $l_{\max}$, S, and ϖ are the maximum edge, line spacing, and linewidth of the polygon inductor, respectively.

$$\omega_r = (E_L + E_C)/\hbar \quad \text{for } \beta=\pi. \tag{4b}$$

Equation (4) indicates that the electron starts resonating to form a standing wave as long as its energy is equal to the kinetic energy plus the total energy lost in the corner field scattering.

This integral model is examined by comparing with the contemporary three-dimensional finite element calculation via the ANSOFT-HFSS simulator[15] whose accuracy is experimentally validated first. Figure 1 shows good S-parameter matches between the measurement result and high frequency structure simulator (HFSS) simulation in a Smith chart for the case of two-port 3.5 turns rectangular micromachined spiral inductors [Fig. 1(a)]. The silicon substrate underneath the inductor has been removed. The detail fabrication and measurement of the spiral inductors have been reported in a previous publication.[16] Although our measurement range is only up to 20 GHz due to the experimental limitation, Lee *et al.* have shown that the HFSS can provide trustworthy results in the frequency prediction.[17] A variety of two-port polygonal spiral microinductors including rectangular, octagonal, and circular inductors is utilized to verify the universality of the integral model as shown in Fig. 2. For a circular spiral inductor, its geometry is treated as infinite amount of minute corner sectors with the angle of π that are serially linked together, so its self-resonant frequency can be determined by Eqs. (3b) and (4b). In comparison with the self-resonant frequencies of the spiral inductors calculated by means of this model and the ANSOFT-HFSS, less than 6% deviation has been found in Table I–III, respectively. The results indicate that a

TABLE I. Case A: Rectangular spiral inductor.

	Number of turns (n)				
Comparisons	1.5	2.5	3.5	4.5	5.5
ω_r for HFSS (GHz)	39.7	27.7	22.7	20.9	19.8
ω_r for model (GHz)	38.6	28.6	23.9	21.4	19.9

TABLE II. Case B: Octagonal spiral inductor.

	Number of turns (n)				
Comparisons	1.5	2.5	3.5	4.5	5.5
ω_r for HFSS (GHz)	42.7	29.5	23.6	21.0	19.9
ω_r for model (GHz)	41.0	30.3	24.9	21.9	20.1

very close prediction can be realized using the integral model.

Moreover, the two different calculations have been compared in terms of the CPU processing time. The integral model is first programmed using MATLAB simulator.[18] The comparison is then done in the same computer with the equipments of 3.4 GHz dual CPUs with DDR2 2048 Mbytes random access memories. About 6400 times of CPU time can be saved if the SRF is predicted using this integral model for a 5.5 turn octagonal spiral inductor. The model can indeed provide a fast and accurate prediction. It is noted that the model can be also easily utilized to construct an equivalent lumped circuit model of spiral inductor for circuit designers while the inductance (L) and the self-parasitic capacitance (C) of inductor are derived by Greenhouse based approach[19] and the SRF from our model.

Substrate coupling effect is excluded in this letter at this moment. The comparison is only based on the inductor without having substrate underneath. Although such a design has been proposed for high performance RFICs due to the high Q characteristic of the inductor,[20,21] we think that the integral can be further modified for general on-chip inductors by considering the interaction between the electric dipoles inside the dielectric layer underneath the inductor and the free electrons inside the inductor.

In summary, the analysis creates a closed-form integral model which could well predict the SRF of a two-port polygonal micromachined spiral inductor. The model could provide not only a quick and accurate prediction but also a mathematically convenience for the optimal inductor design in physical sense.

TABLE III. Case C: Circular spiral inductor. Around 62000 tetrahedral meshes with an average size of 0.15 μm are utilized for the HFSS analyses. The analysis error is controlled below 0.005%. The mesh number will be slightly different in each case due to the geometrical difference. $l_{\max}=300$ μm, $\varpi=15$ μm, and $S=5$ μm.

	Number of turns (n)				
Comparisons	1.5	2.5	3.5	4.5	5.5
ω_r for HFSS (GHz)	43.3	30.5	24.6	21.9	20.7
ω_r for model (GHz)	41.0	30.6	25.8	23.2	21.7

This work was supported by the NSC 94-2220-E-009-002 project and in part by MediaTek research center and FY 95 ITRI/STC/JDRC at National Chiao Tung University.

[1] H. Lakdawala, X. Zhu, H. Luo, S. Santhanam, L. R. Carley, and G. K. Fedder, IEEE J. Solid-State Circuits **37**, 394 (2002).
[2] M. Grozing, A. Pascht, and M. Berroth, J. Spectrosc. Soc. Jpn. **50**, 1927 (2001).
[3] B. Piernas, K. Nishikawa, K. Kamogawa, T. Nakagawa, and K. Araki, IEEE Trans. Microwave Theory Tech. **50**, 4942 (2002).
[4] H. Y. Tsui and J. Lau, IEEE Radio Frequency Integrated Circuits (RFIC) Symposium, 8-10 June 2003 (IEEE, New York, 2003), p. 243.
[5] G.-A. Lee, M. Megahed, and F. De Flaviisl, J. Spectrosc. Soc. Jpn. **1**, 527 (2003); **3**, 1621 (2002).
[6] J. Sieiro, J. M. Lopez-Villegas, J. Cabanillas, J. A. Osorio, and J. Samitier, IEEE Radio Frequency Integrated Circuits (RFIC) Symposium (IEEE, New York, 2001), p. 121.
[7] J. C. Rautio, IEEE Trans. Microwave Theory Tech. **52**, 257 (2004).
[8] C. A. Brau, *Modern Problems in Classical Electrodynamics* (Oxford University Press, New York, 2004), Vol. 4, p. 240.
[9] J. D. Jackson, *Classical Electrodynamics* (Wiley, New York, 1998), Vol. 3, p. 104.
[10] G. B. Arfken and H. J. Weber, *Mathematical Methods for Physicists* (Academic, San Diego, 2001), Vol. 17, p. 1017
[11] A. S. Kronfeld and B. Nižić, Phys. Rev. D **44**, 3445 (1991).
[12] F. J. Federspiel, R. A. Eisenstein, M. A. Lucas, B. E. MacGibbon, K. Mellondorf, A. M. Nathan, A. O'Neill, and D. P. Wells, Phys. Rev. Lett. **67**, 1511 (1991).
[13] C. C. Chen, J. K. Huang, and Y. T. Cheng, IEEE Microw. Wirel. Compon. Lett. **15**, 778 (2005).
[14] J. Y. Park and M. G. Allen, IEEE Trans. Adv. Packag. **22**, 207 (1999).
[15] Ansoft, ANSOFT-HFSS, Version 9.0, http://www.ansoft.com/products/hf
[16] J. W. Lin, C. C. Chen, and Y.-T. Cheng, IEEE Trans. Electron Devices **52**, 1489 (2005).
[17] G.-A. Lee, M. Megahed, and F. De Flaviis, IEEE MTT-S Int. Microwave Symp. Dig. **3**, 1621 (2002).
[18] Mathwork, MATLAB, Version 7.0.4, http://www.mathworks.com/products/matlab/
[19] S. Jenei, B. K. J. C. Nauwelaers, and S. Decoutere, IEEE J. Solid-State Circuits **37**, 77 (2002).
[20] H. Lakdawala, X. Zhu, X. H. Luo, S. Santhanam, L. R. Carley, and G. K. Fedder, IEEE J. Solid-State Circuits **37**, 394 (2002).
[21] J. Hongrui, Y. Wang, J.-L. A. Yeh, and N. C. Tien, J. Spectrosc. Soc. Jpn. **48**, 2415 (2000).